Using active resonator impedance matching for shot-noise limited, cavity enhanced amplitude modulated laser absorption spectroscopy

Jong H. Chow, Ian C. M. Littler, David S. Rabeling
David E. McClelland and Malcolm B. Gray

Centre for Gravitational Physics, Faculty of Science, The Australian National University, Canberra, ACT 0200, Australia

jong.chow@anu.edu.au

Abstract: We introduce a closed-loop feedback technique to actively control the coupling condition of an optical cavity, by employing amplitude modulation of the interrogating laser. We show that active impedance matching of the cavity facilitates optimal shot-noise sensing performance in a cavity enhanced system, while its control error signal can be used for intra-cavity absorption or loss signal extraction. We present the first demonstration of this technique with a fiber ring cavity, and achieved shot-noise limited loss sensitivity. We also briefly discuss further use of impedance matching control as a tool for other applications.

OCIS codes: (120.6200) Spectrometers and spectroscopic instrumentation; (300.6380) Spectroscopy, modulation; (300.1030) Absorption Spectroscopy; (230.5750) Resonators.

References and links

1. J. Ye, L.-S. Ma and J. L. Hall, "Ultrasensitive detections in atomic and molecular physics: demonstration in molecular overtone spectroscopy," J. Opt. Soc. Am. B, **15**, 6-15 (1998).
2. W. Demtröder, *Laser Spectroscopy, Basic Concepts and Instrumentation*, 2nd Enlarged Ed., (Springer-Verlag, Germany, 2003).
3. R. van Zee and J. Patrick Looney, eds., *Cavity-Enhanced Spectroscopies:Experimental Methods in the Physical Sciences*, (Academic Press, California, USA, 2002) Vol. 40.
4. T. McGarvey, A. Conjusteau and H. Mabuchi, "Finesse and sensitivity gain in cavity-enhanced absorption spectroscopy of biomolecules in solution," Opt. Express, **14**, 10441-10451 (2006).
5. A. E. Siegman, *Lasers* (University Science, Mill Valley Calif., 1986).
6. R. W. P. Drever, J. L. Hall, F. V. Kowalski, J. Hough, G. M. Ford, A. J. Munley, and H. Ward, "Laser phase and frequency stabilization using an optical resonator," Appl. Phys. B, **31**, 97-105 (1983).
7. J. H. Chow, M. B. Gray, I. C. M. Littler, and D. E. McClelland, "Spectroscopic detection system and method," Australian Patent Application No. 2007906639.
8. P. R. Saulson, *Fundamentals of Interferometric Gravitational Wave Detectors*, (World Scientific Publishers, Singapore, 1994).
9. M. Cai, O. Painter, and K. J. Vahala, "Observation of critical coupling in a fiber taper to a silica-microsphere whispering-gallery mode system," Phys. Rev. Lett. **85**, 74-77 (2000).
10. D. S. Rabeling, et. al., "Experimental demonstration of impedance matching locking and control for coupled resonators," manuscript under preparation.

#93886 - $15.00 USD Received 14 Mar 2008; revised 2 May 2008; accepted 9 May 2008; published 14 May 2008

1. Introduction

Optical absorption spectroscopy is an active branch of research which finds important applications in biochemical sensing. The fundamental challenge is to attain ever lower detection thresholds. Towards this end, optical resonators are excellent transducers for amplifying the effects of small optical absorption and loss. Methodologies adopting radio-frequency modulation for detecting vibrational overtones of gas-phase molecules have recorded shot-noise limited performance at $1.5\times10^{-13}/\sqrt{\text{Hz}}$ [1]. These frequency modulation (FM) spectroscopy techniques are powerful for species with absorption linewidths of ~ 1 GHz. For molecules in liquids, on the other hand, the spectral line is greatly broadened with a homogeneous profile. This can be compounded by overlapping of profiles from different spectral lines, resulting in an absorption continuum which can extend up to tens of THz [2]. With conventional laser modulation technology, this absorption continuum appears as a broadband loss to the spectral components of the frequency modulated laser, which renders frequency modulation spectroscopy techniques ineffective.

The most widely investigated cavity enhanced technique suitable for broadband loss is time-domain ring-down spectroscopy [3]. However, they typically yield poor sensitivity due to the limited optical duty cycle and the large effective noise bandwidth.

Recently McGarvey et al [4] have proposed a highly sensitive alternative for measuring absorption in liquids, where the laser is locked on resonance, while the reflected power is continually monitored for changes in cavity loss. This frequency domain solution is potentially capable of reaching cavity enhanced, shot-noise limited loss sensitivity given by the well-known expression [1]

$$(\alpha l)_{\text{SN}} = \frac{\pi}{2\mathfrak{F}} \times \sqrt{\frac{2eB}{\eta P_{\text{opt}}}} \tag{1}$$

where α is the absorption coefficient in units of (cm^{-1}); l is the single-pass sample length; $2\mathfrak{F}/\pi$ is the effective bounce number of the resonator; $\mathfrak{F}$ is the cavity finesse; η is the photodetector responsivity; B is the detection bandwidth; and P_{opt} is the optical power incident on the optical resonator. In their experiment, an absorption threshold of $3.4\times10^{-8}/\sqrt{\text{Hz}}$ was achieved with $\mathfrak{F}$ of 3.4×10^{4}. This sensitivity, although preliminary, was reported to be a factor of ~ 200 above the shot-noise limit.

In this paper we introduce an active cavity impedance matching feedback control methodology for a proposed shot-noise limited, cavity enhanced amplitude modulated laser absorption spectroscopy (CEAMLAS) system. It utilizes amplitude modulation (AM) interferometry with closed-loop measurements. We show that this technique can be used to ensure optimal shot-noise sensing performance in a cavity enhanced measurement, while facilitating intra-cavity absorption or loss measurement. We present results for the first experimental demonstration of this technique with a fiber ring cavity, which shows shot-noise limited loss sensitivity. Finally, we discuss some broader applications of this active impedance matching technique.

2. Active impedance matching of an optical cavity

To aid in understanding the CEAMLAS technique, we consider a linear Fabry-Perot cavity illustrated by Fig. 1, consisting of an input coupler mirror and an output coupler mirror with reflectivities $R_1(V_{\text{act}})$ and R_2 respectively. We assume that $R_1(V_{\text{act}})$ can be varied by applying a voltage, V_{act}, to its actuator. For small signals of V_{act}, $R_1(V_{\text{act}})$ can be approximated as linearly dependent on V_{act}. The mirrors have transmissivities $1-R_1(V_{\text{act}})$ and $1-R_2$, and there is an intra-cavity single-pass absorption αl, besides which the cavity is assumed to be loss-

#93886 - $15.00 USD Received 14 Mar 2008; revised 2 May 2008; accepted 9 May 2008; published 14 May 2008

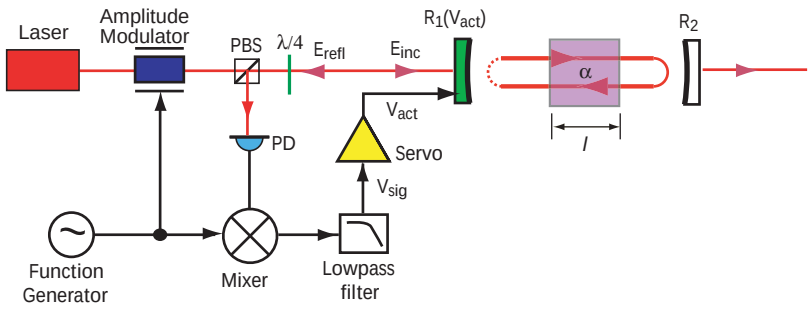

Fig. 1. Conceptual schematic of the CEAMLAS technique with a free space linear cavity. The reflectivity of the input coupler is variable via an actuation voltage. It is used to actively impedance match the cavity with a feedback control loop. The error signal for this control loop is provided by amplitude modulation of the laser and demodulation of the reflected light.

less. We will show that by interrogating this cavity with amplitude modulated laser light, signal extraction of shot-noise limited absorption sensitivity can be achieved.

2.1. *Coupling conditions of an optical cavity*

For a continuous wave (CW) laser incident on this optical cavity, on resonance its reflection field response is purely real, and can be given by

$$r_{\text{res}} = \frac{r_1 - r_2 e^{-\alpha l}}{1 - r_1 r_2 e^{-\alpha l}}. \tag{2}$$

The amplitude reflection coefficients r_1 and r_2 correspond to $\sqrt{R_1(V_{\text{act}})}$ and $\sqrt{R_2}$ of the two cavity mirrors, keeping in mind that r_1 is variable by the actuation voltage V_{act}.

When $r_1 > r_2 e^{-\alpha l}$, the cavity is considered "under-coupled", while it is "over-coupled when $r_1 < r_2 e^{-\alpha l}$. For the special condition when $r_1 = r_2 e^{-\alpha l}$, the resonator is *"impedance-matched"* [5]. This is when the reflected power from the cavity is exactly zero on resonance.

2.2. *Laser amplitude modulation and demodulated error signals*

We define the optical electric field amplitude as $E_0 = Ae^{-i\omega_0 t}$, such that the optical power P_{opt} is given by

$$P_{\text{opt}} = |E_0|^2 = A^2. \tag{3}$$

When this laser is amplitude modulated sinusoidally at a radio frequency (RF) ω_m (rad/s), as illustrated in Fig. 1, its modulated field can be described by

$$E_{\text{inc}} = Ae^{-i\omega_0 t}\left[1 + \frac{\beta}{2}e^{+i\omega_m t} + \frac{\beta}{2}e^{-i\omega_m t}\right], \tag{4}$$

where β is the modulation depth. In writing Eq. 4 we have assumed that $\beta << 1$, and therefore the optical power in the carrier $P_c \approx 1$. This modulated laser is used to interrogate a resonant cavity as illustrated in Fig. 1. The polarization beamsplitter (PBS) and quarter-wave plate ($\lambda/4$) combination ensures that all the reflected light is received by the photodetector.

For the purpose of the following discussion, we will assume that the laser carrier is resonant with the optical cavity. This is typically facilitated by an active feedback control loop,

#93886 - $15.00 USD Received 14 Mar 2008; revised 2 May 2008; accepted 9 May 2008; published 14 May 2008

such as the Pound-Drever-Hall (PDH) frequency locking [6] technique. When the laser carrier frequency ω_0 is resonant, the optical field reflected from the cavity can be expressed as

$$E_{\rm refl} \quad = \quad Ae^{-i\omega_0 t}\Big[\frac{r_1 - r_2 e^{-\alpha l}}{1 - r_1 r_2 e^{-\alpha l}} + \frac{\beta}{2}e^{+i\omega_m t} + \frac{\beta}{2}e^{-i\omega_m t}\Big]. \tag{5}$$

In Eq. 5, it is assumed that the modulation frequency ω_m is much wider than the resonance full-width half-maximum (FWHM) of the cavity. All the power in the modulation sidebands are hence reflected, while the carrier experiences the reflection response of the cavity, as described by Eq. 2.

This reflected light is received by a photodetector (PD) and its RF output signal demodulated by the local oscillator. After low-pass filtering to obtain only the DC terms, the resultant AM error signal at the mixer output can be written as

$$V_{\rm sig} \quad \approx \quad \eta\beta P_{\rm opt} R_{\rm pd} \frac{r_1 - r_2 e^{-\alpha l}}{1 - r_1 r_2 e^{-\alpha l}}, \tag{6}$$

where η is the photodetector responsivity; and $R_{\rm pd}$ is the trans-impedance gain of the photodetector (Ω).

It is clear from Eq. 6 that $V_{\rm sig}$ provides a measure of the cavity coupling condition. Its polarity is positive when the cavity is under-coupled; negative when over-coupled, and zero when it is impedance-matched. The DC component of $V_{\rm sig}$ can be used to measure the steady-state absorption αl, while its AC component can be used to detect small changes in intra-cavity absorption $\Delta(\alpha l)$.

Furthermore, this error signal can be amplified with a servo to provide a feedback voltage $V_{\rm act}$, which is used to actuate $R_1(V_{\rm act})$ to keep the cavity impedance-matched in an active control loop. We will discuss in Sect. 3 the advantages of active impedance matching in cavity-enhanced absorption measurements.

3. The shot-noise equivalent minimum detectable absorption limit

To calculate the smallest detectable absorption signal at the shot-noise limit, it is necessary to consider a small change in $V_{\rm sig}$ due to a small change $\Delta(\alpha l)$ at a steady-state DC αl. This small voltage signal is compared with the shot-noise voltage at a signal-to-noise ratio of unity, to obtain an expression for the theoretical shot-noise limit for absorption.

3.1. General expression for shot-noise limited absorption sensitivity

For a small change $\Delta(\alpha l)$ from an initial DC value of αl, Eq. 6 yields the small signal approximation

$$\Delta V_{\rm sig} \quad \approx \quad \eta\beta P_{\rm opt} R_{\rm pd}\left[\frac{r_2 e^{-\alpha l}}{1 - r_1 r_2 e^{-\alpha l}} - \frac{(r_1 - r_2 e^{-\alpha l})(r_1 r_2 e^{-\alpha l})}{(1 - r_1 r_2 e^{-\alpha l})^2}\right]\Delta(\alpha l). \tag{7}$$

By considering the total reflected power $P_{\rm refl} = |E_{\rm refl}|^2$ detected by the photodetector, the shot-noise voltage at the mixer output can be written as

$$V_{\rm SN} \quad = \quad R_{\rm pd}\sqrt{e\eta P_{\rm opt}\Big[\Big(\frac{r_1 - r_2 e^{-\alpha l}}{1 - r_1 r_2 e^{-\alpha l}}\Big)^2 + \frac{\beta^2}{2}\Big]}, \tag{8}$$

where we have assumed a detection bandwidth of 1 Hz. Using Eqs. 7 and 8, by assuming

#93886 - $15.00 USD Received 14 Mar 2008; revised 2 May 2008; accepted 9 May 2008; published 14 May 2008

signal-to-noise ratio of unity, we obtain

$$\Delta(\alpha l)_{\min} = \frac{(1-r_1 r_2 e^{-\alpha l})^2}{[(1-r_1 r_2 e^{-\alpha l})(r_2 e^{-\alpha l}) - (r_1 - r_2 e^{-\alpha l})(r_1 r_2 e^{-\alpha l})]\beta} \times \sqrt{\frac{e}{\eta P_{\text{opt}}}\left[\left(\frac{r_1 - r_2 e^{-\alpha l}}{1 - r_1 r_2 e^{-\alpha l}}.\right)^2 + \frac{\beta^2}{2}\right]}. \quad (9)$$

Equation 9 provides a general expression for the minimum detectable intra-cavity absorption as a function of mirror reflectivities in high finesse cavities, using RF AM laser interrogation.

3.2. *Absorption sensitivity and cavity coupling*

It can be seen from Eq. 8 that, for a given laser optical power and modulation depth, the minimum shot-noise of the system is achieved when $r_1 = r_2 e^{-\alpha l}$, or when the cavity is exactly *impedance-matched*. By further assuming that both r_1, r_2 approach unity, and αl is small, Eq. 9 can be reduced to Eq. 1 as the fundamental limit.

We note that for a system dominated by shot noise, the limit of Eq. 1 is only reached when the modulation depth is vanishingly small and $P_c \approx 1$. Any portion of the carrier power converted to the sidebands would lead to a slight loss of sensitivity for a fixed total optical power [3]. In practice, non-optical noise sources, such as detector electronic noise, require a finite modulation depth. The resulting sensitivity will hence be marginally worse than the value predicted by Eq. 1.

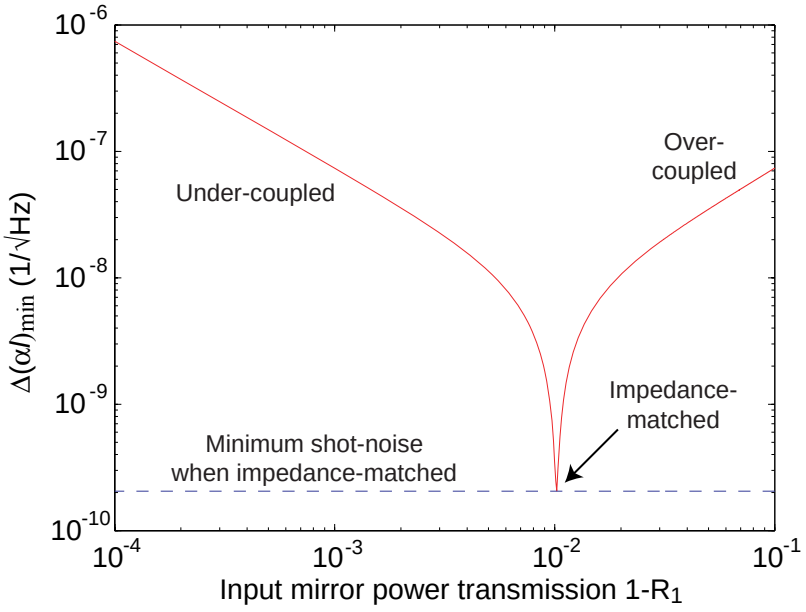

Fig. 2. Theoretical minimum detectable shot-noise limited absorption vs. different cavity coupling conditions. The cavity coupling is varied by varying the input coupler reflectivity. The minimum shot-noise occurs when the cavity is impedance-matched, when $r_1 = r_2 e^{-\alpha l}$. For this plot, we have assumed $R_2 = 0.99$; $\alpha l = 1 \times 10^{-4}$; $\beta = 0.01$; $\eta = 1$(A/W); and $P_{\text{opt}} = 200$ (μW)

The degradation of absorption sensitivity away from the impedance-matched condition can

#93886 - $15.00 USD Received 14 Mar 2008; revised 2 May 2008; accepted 9 May 2008; published 14 May 2008

be illustrated by Fig. 2, where we plot the theoretical shot-noise sensitivity as a function of input mirror transmissivity $1-R_1$. For this plot, we have assumed $R_2 = 0.99$; $\alpha l = 1\times10^{-4}$; $\beta = 0.01$; $\eta = 1$(A/W); and $P_{\rm opt} = 200$ (μW). On either side of impedance matching, the reflected power of the carrier is non-zero, and degrades the shot noise voltage at the mixer output, as governed by Eq. 8. Figure 2 shows that when the cavity is impedance-matched, $\Delta(\alpha l)_{\rm min}$ reaches its lowest value, which is the operating condition for optimal absorption sensitivity. The dramatic increase in $\Delta(\alpha l)_{\rm min}$ on either side of an impedance-matched cavity shows the necessity to implement an active feedback control loop to keep the cavity at the optimal operating condition.

Since the impedance-matched absorption sensitivity is governed by Eq. 1, the minimum detectable $\Delta(\alpha l)_{\rm min}$ can be improved by either increasing the optical power $P_{\rm opt}$, or increasing the cavity finesse $\mathfrak{F}$, where $\mathfrak{F}$ is a function of mirror reflectivities and the DC absorption αl.

3.3. Absorption sensitivity with increased sample length

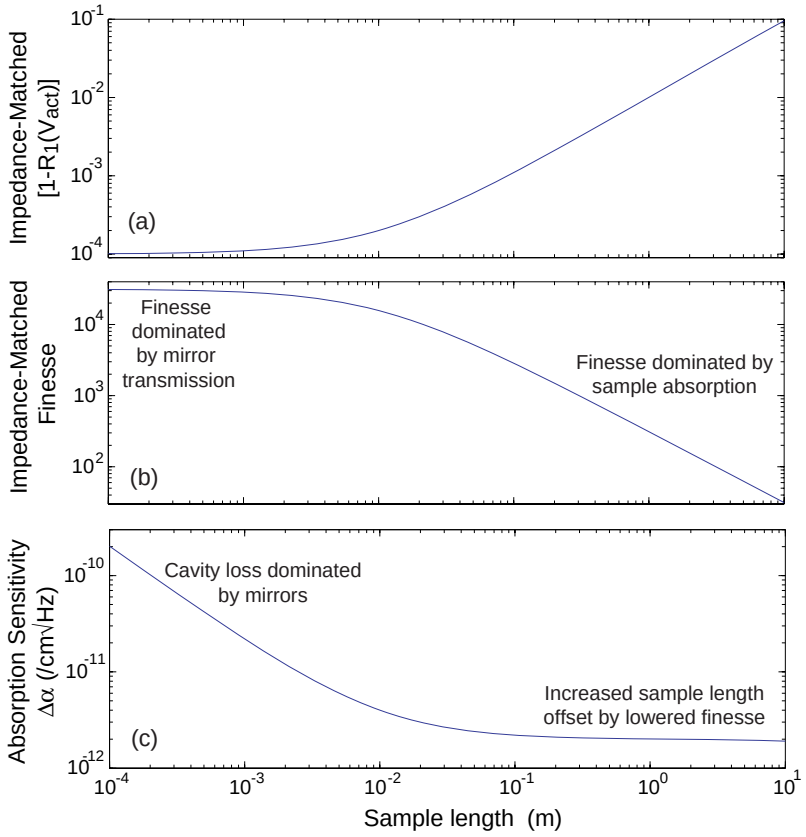

Fig. 3. The effect of increasing absorbing sample length on: a) the transmissivity of the input coupler to keep the cavity impedance-matched; b) the impedance-matched cavity finesse; and c) the theoretical minimum detectable shot-noise limited absorption coefficient.

It is also instructive to see how the minimum detectable absorption coefficient change $(\Delta\alpha)_{\rm min}$ (/cm$\sqrt{\rm Hz}$) is affected by the sample length l. Figure 3 displays three plots as the sam-

#93886 - $15.00 USD Received 14 Mar 2008; revised 2 May 2008; accepted 9 May 2008; published 14 May 2008

ple length l is increased from 10^{-4} to 10^{1} (m), while the cavity is kept impedance-matched: (a) the input mirror reflectivity $R_1(V_{\text{act}})$ necessary to keep the cavity impedance-matched; (b) the decrease in cavity finesse as l increases; and (c) the corresponding absorption coefficient sensitivity with increase in l. For these theoretical plots, we have assumed R_2 to be 0.9999; and the DC value of α to be 5×10^{-5} (cm^{-1}).

For very short sample lengths in Fig. 3(a), the cavity loss is dominated by the output mirror, and hence the change in $R_1(V_{\text{act}})$ required to keep the cavity impedance-matched as l changes is relatively small. But as the sample length increases, the loss due to absorption becomes significant, and $R_1(V_{\text{act}})$ needs to be adjusted accordingly. As losses due to input mirror transmission and sample absorption increase, a corresponding decrease in finesse $\mathfrak{F}$ can be expected, as shown in Fig. 3(b).

More importantly, at very short sample lengths where the DC absorption αl is small compared with mirror transmission, the absorption coefficient sensitivity in this extreme improves with increased sample length, such that $(\Delta\alpha)_{\min} \propto 1/l$, as shown in Fig. 3(c). In the regime where sample absorption is significant, however, $(\Delta\alpha)_{\min}$ levels off to approach a constant value, as any potential sensitivity gain from increased sample interaction is offset by the degradation in cavity finesse $\mathfrak{F}$.

Figure 3 shows that for a given DC value of α, increasing the finesse of the cavity (by increasing R_1, R_2, and/or decreasing l) alone does not necessarily improve absorption sensitivity. For a given DC value of α, the mirror reflectivities and sample length should ideally be designed to operate in the flat region similar to that in Fig. 3(c) for optimal performance. Increasing the cavity finesse would only improve absorption sensitivity of this flat region if the DC value of α is also decreased.

4. Experimental demonstration of CEAMLAS

4.1. Experimental setup

To demonstrate the CEAMLAS technique experimentally, we set up a fiber ring cavity as illustrated by the dashed box in Fig. 4. Each of the two couplers used a pair of evanescently coupled fibers whose separation was actuated via a piezo-electric transducer (PZT) to give a variable fiber coupler with coupling ratio from 0 to 1, dependent on the applied voltage. The input Coupler A had variable electric field coupling coefficient u, as shown by the solid box inset in Fig. 4. The variable Coupler B introduced broadband intracavity loss, associated with the coupling coefficient v. This ring cavity emulated the linear cavity illustrated in Fig. 1, where u was equivalent to r_1 of the input coupler; while v was equivalent to $e^{-\alpha l}$ related to an absorbing medium. Hence Coupler B can be used to emulate variable intra-cavity absorption via its PZT, while Coupler A was used for active impedance matching of the ring cavity, by actuating on its PZT in a feedback control loop.

By substituting these equivalent coefficients into Eq. 6, we obtain the expression for the AM error signal for this setup

$$V_{\text{sig}} \approx \eta\beta P_{\text{opt}} R_{\text{pd}} \frac{\Delta r}{1-uv}, \tag{10}$$

where $\Delta r = u - v$ is the coupling ratio difference between u and v.

A tunable commercial fiber laser at 1550 nm, with a nominal linewdith of 2 kHz and P_{opt} of 100μW, was used to interrogate the fiber ring cavity. The laser was attached to a PZT, which stretch-tuned its frequency with an applied voltage. This laser was phase modulated (PM) at 69 MHz by a function generator to implement the PDH frequency locking loop, and amplitude modulated at 20 MHz with a second function generator for the impedance matching locking loop. Both PM and AM were implemented with a JDSU waveguide modulator device.

#93886 - $15.00 USD Received 14 Mar 2008; revised 2 May 2008; accepted 9 May 2008; published 14 May 2008

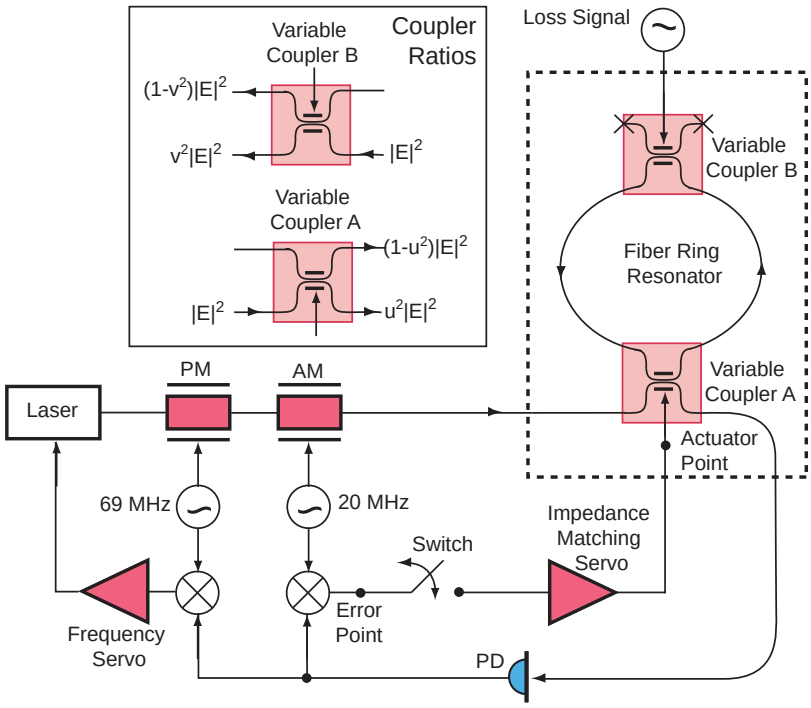

Fig. 4. The experimental schematic for the CEAMLAS demonstration. The fiber ring cavity has a variable input Coupler A for impedance-matching, while Coupler B introduces cavity loss to emulate intra-cavity absorption. The phase modulation and PDH frequency locking system ensure that the laser carrier is held on cavity resonance. The amplitude modulated carrier can then interrogate the impedance coupling condition of the cavity. The "error point" yields the open-loop cavity loss measurement while the "actuator point" yields the closed-loop cavity loss measurement.

The modulated laser light was then used to interrogate the fiber ring cavity, and light reflected from the cavity was received by a photodetector (PD). The RF electronic output from the photodetector was demodulated respectively by the two local oscillators to provide the PDH and impedance matching error signals.

4.2. PM and AM error signals by scanning laser frequency

In open-loop operation, Fig. 5 shows oscilloscope traces recorded as the laser frequency was scanned across two fiber ring cavity resonances. Figure 5(a) shows the optical power reflected off the fiber ring cavity and incident on the photodetector as shown in Fig. 4. The free spectral range of this cavity was $\sim$ 400 MHz, which was consistent with a physical fiber length of $\sim$ 0.5 m for the ring cavity. Its resonance FWHM was $\sim$ 6.7 MHz, for a modest finesse of $\sim$ 60. The cavity was close to impedance matching and the reflected power dropped towards zero on resonance. Due to the optical power in both PM and AM sidebands, the reflected power on resonance can never drop identically to zero. The corresponding demodulated PDH error signal derived from PM modulation is displayed in Fig. 5(b).

The lower trace Fig. 5(c) shows the demodulated AM error signal as the laser frequency was scanned. As the carrier was scanned through resonance, the AM error signal crossed and dipped

#93886 - $15.00 USD Received 14 Mar 2008; revised 2 May 2008; accepted 9 May 2008; published 14 May 2008

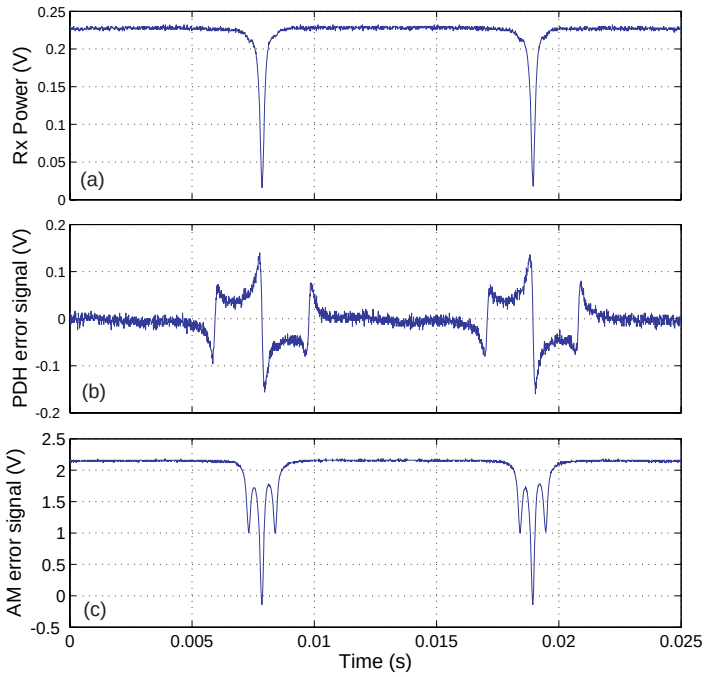

Fig. 5. (a) The optical power reflected off the fiber ring cavity as the laser frequency is scanned across resonance. (b) The PDH error signal that is used to lock the laser to resonance. This relies on 69MHz phase modulation sidebands. (c) the AM error signal used to measure cavity loss. The AM sidebands are at a frequency of 20MHz.

below zero. Exactly on resonance, the error signal was close to zero with a small negative value. This indicates that this cavity was marginally over-coupled. The two satellite error signals in Fig. 5(b), and two satellite peaks in Fig. 5(c), on either side of each resonance, are consistent with the PM and and AM sidebands at frequencies 69 MHz and 20 MHz, respectively.

From Fig. 5 we see that when the laser was locked exactly to cavity resonance, the AM error signal would yield a negative DC voltage with the above cavity coupling conditions. This DC impedance locking error signal was governed by Eqn. 10.

4.3. Open-loop impedance matching error signal when frequency locked

To keep the laser carrier on resonance, the PDH frequency locking control loop was then closed. The demodulated PDH error signal was used by the frequency servo to provide a feedback voltage to the laser PZT actuator, thereby keeping the laser resonant, so that the system was immune to thermal, mechanical and acoustic perturbations to the ring cavity.

Once the laser was locked to a cavity resonance, the input coupler ratio was scanned whilst recording both the cavity output optical power and the AM error signal. This is plotted in Fig. 6 where the left-hand vertical axis scales the cavity output optical power transmitted via Coupler A; the right-hand vertical axis scales the AM error signal. As can be seen, the AM error signal crosses zero, where the output power is minimum. We note also that the error signal around this impedance-matched condition is linear.

On either side of this optimum point, the transmitted power increased as the impedance matching deteriorates. At the extreme edges of Fig. 6, the AM error signal saturated, indicating

#93886 - $15.00 USD Received 14 Mar 2008; revised 2 May 2008; accepted 9 May 2008; published 14 May 2008

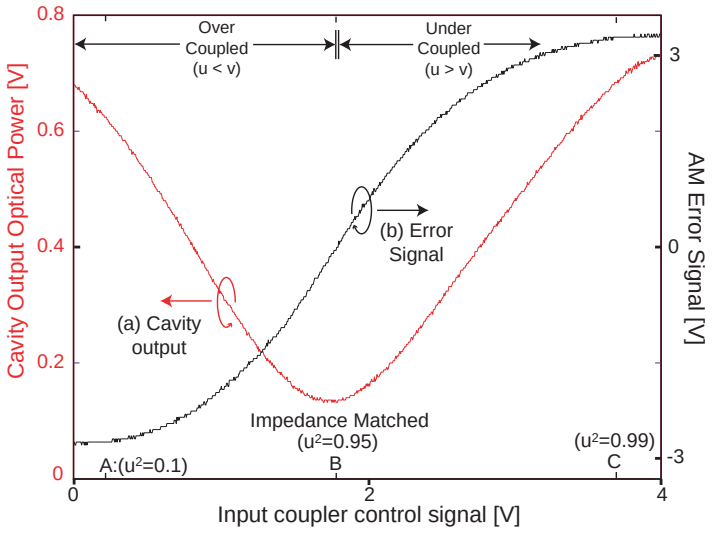

Fig. 6. Experimental plots showing: (a) The fiber ring cavity output optical power while the ratio u of input Coupler A is scanned; (b) the corresponding cavity loss error signal recorded at the "error point" of Fig. 4. The coupling ratio for Coupler B was held constant at $v^2 = 0.95$.

that the on resonance reflectivity of the carrier approached unity for both the over-coupled (u^2 approaches zero on the left hand side) and the under-coupled (u^2 approaches unity on the right hand side) extremes.

4.4. Closed-loop measurements when frequency locked

Before the switch in Fig. 4 was closed, the variable Coupler A was first DC tuned so that the fiber ring cavity was impedance-matched, corresponding to the zero-crossing of the open-loop impedance matching AM error signal. This ensured that the system was operating at its optimal sensitivity.

After the switch was closed, closed-loop measurements could be made at the "actuator point" in Fig. 4 for signals at frequencies where the servo gain was large; the low frequency range extending down to DC. For fast cavity loss processes above the unity gain bandwidth of the impedance servo, the "error point" of Fig. 4 provided an effective "open-loop" error signal readout.

A time-varying loss signal at 1.5 Hz was injected into the fiber ring cavity using variable Coupler B of Fig. 4. The AM error signal, measured at the error point of Fig. 4, then yielded the real time readout of the injected cavity loss. Figure 7(a) shows the resulting AM error signal, while Fig. 7(b) plots the corresponding output optical power through Coupler A. The impedance matching AM error signal was seen to yield a high signal-to-noise readout of the loss. However, the output optical power yielded no first order signal, while a small, noisy second order signal can just be discerned in Fig. 7(b).

Figure 7 demonstrates a major advantage of this RF cavity interrogation technique: whilst measuring the reflected optical power yields no first order signal at the impedance matched point, the AM error signal reaches it's maximum slope at this point and yields a highly sensitive read out of both cavity impedance and cavity loss.

#93886 - $15.00 USD Received 14 Mar 2008; revised 2 May 2008; accepted 9 May 2008; published 14 May 2008

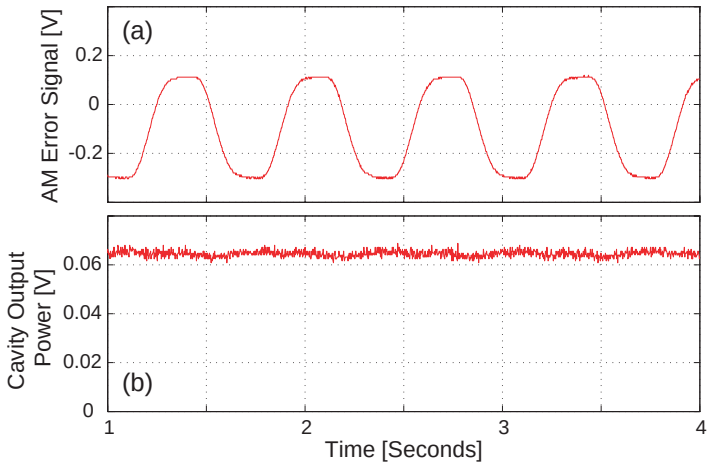

Fig. 7. (a) The AM error point voltage with a 1.5Hz loss signal injected into variable Coupler B of Fig. 4. (b) The corresponding fiber ring cavity output optical power.

4.5. Absorption sensitivity

Using both the time domain trace recorded in Fig. 7 and the AM error signal trace of Fig. 6, we calibrated the demodulated output voltage at the Error Point illustrated in Fig. 4 in terms of single pass cavity loss per $\sqrt{\text{Hz}}$. Trace A of Fig. 8 plots the Fast Fourier Transform (FFT) of this error signal calibrated as loss sensitivity. The CEAMLAS technique can be seen to reach a sensitivity of $\sim 2\times10^{-9}/\sqrt{\text{Hz}}$ at signal frequencies above $\sim$ 10 Hz. This approached the shot-noise limited sensitivity of $1.5\times10^{-9}/\sqrt{\text{Hz}}$ predicted by Eq. 1 for our experimental parameters ($\mathfrak{F}=60$, $P_{\text{opt}}=100\ \mu$W, $\lambda=1550$ nm, $\eta=1$ A/W). Trace C of Fig. 8 plots the electronic noise while trace B is the sum of both shot noise and electronic noise, hence resulting in "$1/f$" electronic noise dominating at low frequencies.

The modest finesse of 60 for this fiber ring cavity was dominated by losses in the couplers and fiber splices, which we have neglected in Fig. 4. This limits the shot-noise of our system as governed by Eq. 1. With better cavity design, this limiting loss can be reduced, yielding a higher achievable cavity finesse and improved absorption sensitivity.

5. Broader implications of active impedance matching

Active impedance matching feedback control offers a powerful new tool in sensing and metrology involving optical resonators, by optimizing the shot-noise performance of a system. As a proof-of-principle experiment, we have demonstrated its operation in guided-wave optics using a fiber ring cavity. It can, however, be applied to numerous different kinds of optical resonators [7], including free space cavities, bulk solid etalons, and optical microcavities such as the microtoroid and microsphere resonators. In this section we briefly discuss the broader aspects of active impedance matching and a few of their potential applications.

5.1. Absorption spectroscopy

In addition to optimizing the cavity loss sensitivity, active cavity impedance matching also improves the dynamic range of this technique. With closed-loop operation, the system can track large loss changes within the cavity while actively matching the impedance of the cavity. Under these conditions, the system is limited only by the dynamic range of the actuator-variable input

#93886 - $15.00 USD Received 14 Mar 2008; revised 2 May 2008; accepted 9 May 2008; published 14 May 2008

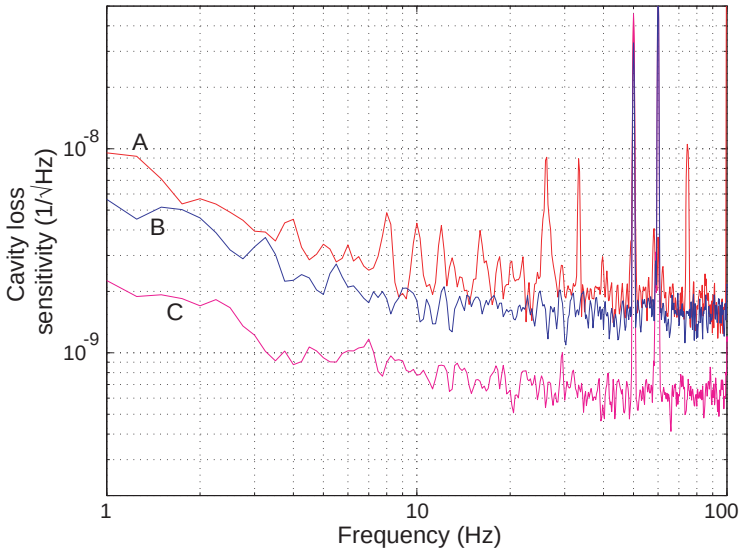

Fig. 8. A) FFT of the error point voltage; B) sum of shot noise and electronic noise; C) the electronic noise spectral density.

coupler and not the linear region of the AM error signal.

Furthermore, when impedance matched, the AM error signal is zero and the loss measurement becomes a ”null” measurement [8]. This leads to immunity to low frequency laser intensity noise, and thus alleviates the need for laser intensity stabilization. In contrast, absorption measurements that rely directly on optical power reflected or transmitted from a cavity cannot distinguish inherent laser intensity fluctuations from the intra-cavity signal.

CEAMLAS can be used for measuring absorption in both gaseous and liquid phase samples, as the amplitude modulation technique does not rely on narrowband differential attenuation of sidebands. For narrowband absorption, it suffices to align the frequency locked laser carrier with the absorption peak. For broadband absorption, CEAMLAS offers the potential to reach absorption sensitivities similar to those attained by phase modulation techniques in gaseous samples [1]. Thus it can also be used for absorption measurements in high clarity solid bulk material, such as ultra-pure fused silica.

5.2. Critical coupling of microcavities

In recent years, microcavities such as microspheres and microtoroids have gained broad interest in quantum optics as well as potential devices for sensing. One of the main challenges in working with these devices is the evanescent coupling of these cavities with tapered optical fibers [9]. For critical coupling (or impedance matching), proper mode-matching is required between the tapered fiber and the microcavity. Just as important for coupling efficiency is the distance between them, since it can change dramatically over a μm. Hence any thermal, mechanical or acoustic perturbations can introduce significant fluctuations in coupling efficiency. This can severely affect the sensing readout, and thus the sensitivity of the device.

Active impedance matching can be used to actuate on the fiber-to-cavity separation. Since the demodulated AM error signal is a direct measure of the coupling condition, it can be used

#93886 - $15.00 USD Received 14 Mar 2008; revised 2 May 2008; accepted 9 May 2008; published 14 May 2008

to actuate the evanescent coupling distance for coupling stabilization and control. Furthermore, when these microcavities are used for loss measurements, the preceding discussions in this paper would indicate that our active impedance matching technique can provide a highly sensitive readout at the optimal shot-noise limit.

5.3. Performance enhancement of interferometric gravitational wave detectors

Active impedance matching offers a technique to optimize power coupling into gravitational wave interferometers in real time, improving the total circulating power and thus enhancing the shot-noise limited measurement performance [10]. This can be done by impedance matching of the power recycled cavity in detectors such as the Laser Interferometer Gravitational-Wave Observatory (LIGO).

In addition, the adoption of active impedance matching offers an alternative shot-noise limited displacement signal extraction technique in these detector configurations. For example, in an impedance-matched power recycled cavity, any gravitational-wave signal would change the differential arm-length of its Michelson interferometer, thereby changing the coupling condition. The impedance matching error signal can then be calibrated to provide an equivalent gravitational-wave readout.

6. Conclusion

We have introduced an active impedance matching technique for a resonant cavity, employing amplitude modulation of an interrogating laser, and showed that it provides optimal shot-noise sensing performance in a cavity enhanced system. We presented the first experimental demonstration of this technique for a fiber ring cavity, and achieved shot-noise limited intra-cavity loss sensitivity. This experiment emulates a cavity enhanced absorption spectroscopy measurement for broadband absorption, as typified by liquid phase samples. Beyond absorption spectroscopy, we have also briefly discussed using active impedance matching as a useful tool for other potential applications, such as critical coupling control and stablization of microcavities, and performance enhancement of gravitational-wave detectors.

Acknowledgments

This research was supported by the Australian Research Council.

#93886 - $15.00 USD Received 14 Mar 2008; revised 2 May 2008; accepted 9 May 2008; published 14 May 2008